AIChE WILEY InterScience DISCOVER SOMETHING GREAT

Analytical Approach for Entropy Generation during a Laser-Pulse Heating Process

B. S. Yilbas
Dept. of Mechanical Engineering, King Fahd University of Petroleum and Minerals, Dhahran, Saudi Arabia

M. Kalyon
Gebze Institute of Technology, Kocdeli, Turkey, and Dept. of Mechanical Engineering, King Fahd University of Petroleum and Minerals, Dhahran, Saudi Arabia

DOI 10.1002/aic.10763
Published online January 10, 2006 in Wiley InterScience (www.interscience.wiley.com).

Laser-pulse heating of engineering surfaces finds application in the metal industries. In general, energy-efficient processing depends on the workpiece and laser-pulse properties. Consequently, investigation into entropy generation during the heating and cooling cycles of the process becomes fruitful. In the present study, analytical solutions for temperature distribution and entropy generation inside the substrate material are presented. Temperature distribution and entropy generation resulting from two different pulses having the same energy content, but different pulse lengths, are computed. The entropy number ratio (ratio of entropy generation number in the heating cycle to entropy generation number in the cooling cycle) is obtained. It is found that entropy generated in the surface region of the substrate material is considerably low because of the small temperature gradient in this region. However, the entropy ratio reaches its maximum in this region, which in turn indicates that entropy generation in the heating cycle is considerably higher than its counterpart in the cooling cycle in this region. © 2006 American Institute of Chemical Engineers *AIChE J,* 52: 1941–1950, 2006

Keywords: analytical solution, laser heating, entropy generation

Introduction

Laser heating of surfaces finds application in the metal industries because of its precision of operation, low cost, and capability for local treatment. In laser processing of metals, two regimes are of interest: conduction-limited heating and non-conduction-limited heating. Conduction-limited heating involves solid heating without any phase change taking place in the substrate material, whereas non-conduction-limited heating occurs when the substrate material undergoes phase change processes during the laser-heating pulse. In general, laser pulses with different pulse lengths and intensities are used in both cases. When the laser pulse irradiates the substrate material, temperature rises during the heating pulse. This can be defined as a *heating cycle*, in which case, energy absorbed from the irradiated field is stored in the substrate material. Once the heating pulse ends, the diffusional energy transport from the surface region to the solid bulk arising from the temperature gradient governs the energy transport process: this can be defined as the *cooling cycle*. Laser-heating applications depend on the efficient coupling of incident energy with the substrate material, which is subjected to laser irradiation. The energy coupling depends on the laser-pulse parameters and the substrate material properties, such as laser wavelength, pulse length and energy, pulse intensity, surface reflectivity, and thermal properties of the substrate material. One method of examining the efficient coupling of laser pulse with the workpiece includes entropy analysis because it provides information on the availability destroyed during the heating process. Consequently, through entropy analysis, a laser pulse that results in less availability destruction can be identified.

A considerable number of research studies were carried out

Correspondence concerning this article should be addressed to B. S. Yilbas at bsyilbas@kfupm.edu.sa.

to explore the laser-heating process. Ready[1] obtained an analytical solution for the temperature increase attributed to the laser-heating pulse. His solution was limited to the heating cycle; the cooling cycle of the heating process was not formulated. Blackwell[2] presented a closed-form solution for temperature distribution including the convection energy transport from the surface during the laser-heating pulse. Lu[3] investigated the laser-heating process resulting from a square-shaped laser beam. He showed that the square-shaped temperature profile was almost the same size as that of the original laser beam and it did not depend on the laser beam power. El-Adawi et al.,[4] who analytically investigated a two-layer system subjected to laser irradiation, indicated that the melting time was dependent on the film's thermal properties. Laser heating of a semi-infinite substrate moving at a constant speed was investigated by Modest and Abaikans,[5] who proposed an analytical solution for the temperature distribution in the region irradiated by a laser beam. Moreover, their analysis was limited to a surface source situation, in which case the workpiece material was totally opaque to the incident beam. Yilbas and Shuja[6] reported on their study of laser conduction-limited heating, in which they correlated the heating duration with the equilibrium distance where energy balance occurred among the energy absorbed, internal energy gain of the substrate material, and conduction losses from the surface vicinity to the solid bulk. The analytical solution for a pulsed laser-heating process arising from a convective boundary condition was obtained by Yilbas and Kalyon.[7] They showed that the pulse parameters had a substantial effect on the temperature profiles, in which case the temperature attained low values as the pulse parameter β increased. Laser-pulse heating arising from an exponentially time decaying pulse was formulated by Yilbas,[8] who indicated that almost steady heating could be possible for frequencies of the order of 1 kHz.

Entropy analysis of the thermal system gives insight into the available energy destroyed in the system when it undergoes different processes. A number of research studies were carried out to explore the entropy production in the thermal system.[9-11] Krane[12] investigated the influence of system parameters on entropy number for a Joulean heater. Bejan[13] studied the second law response to the thermal storage system through examining the destruction of thermodynamic availability. Yilbas,[14] who studied entropy generation during the laser-heating process, indicated that the entropy number changed significantly in the heating and cooling cycles.

As the size of the distance in the solid—where the energy transport takes place—becomes comparable to the interatomic size, the Fourier heat conduction equation fails to predict the temperature increase in the region irradiated by a laser beam.[15] This scenario introduces a nonequilibrium energy transport between the electron and lattice subsystems in the solid.[16] Consequently, thermodynamic irreversibility should be addressed to determine the rate of entropy production.[17-20] However, in the present study, the Fourier heating model is used in the analysis, given that the material, which is subjected to a laser-heating pulse, is considered to be a continuum (that is, the size of the irradiated depth is appreciably in excess of the interatomic spacing). A closed-form solution for temperature distribution in the heating and cooling cycles, using a Laplace transformation method, is presented and an analytical solution for entropy generation arising from a heating pulse is derived.

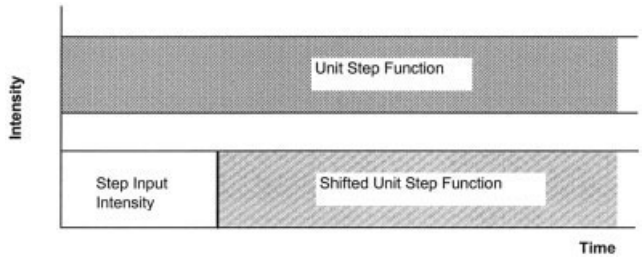

Figure 1. Construction of a step input intensity pulse.

To demonstrate the influence of the laser-pulse properties on the entropy generation in the heating and cooling cycles, two pulses with the same energy content, but different pulse lengths, are considered.

Mathematical Analysis

The governing equations of heat transfer and entropy generation are given under the appropriate subsections. The differential equations for both analyses are nondimensionalized with the appropriate parameters. The closed-form solutions are presented in the nondimensional forms.

Heating analysis

Laser-pulse heating consists of two cycles: heating and cooling. The heating cycle starts with the initiation of the pulse and ends when the pulse intensity reduces to zero. The construction of the laser step intensity pulse can be achieved through subtraction of two unit step functions as shown in Figure 1, that is, the first unit step pulse starts at time $t = 0$, whereas the second unit step pulse (shifted unit step pulse) starts at time Δt (Δt is the pulse length). The difference in both pulses results in the step intensity pulse, that is,

$$SP(t) = 1[t] - 1[t - \Delta t] \tag{1}$$

where

$$1[t] = \begin{Bmatrix} 1, & t > 0 \\ 0, & t < 0 \end{Bmatrix}$$

$$1[t - \Delta t] = \begin{Bmatrix} 1, & t > \Delta t \\ 0, & t < \Delta t \end{Bmatrix} \tag{2}$$

and $SP(t)$ is the step intensity pulse with a unit intensity. The Fourier heat transfer equation for a laser-heating pulse can be written as

$$\frac{\partial^2 T}{\partial x^2} + \frac{I_1 \delta}{k}[C_1 \times SP(t)]e^{-\delta x} = \frac{1}{\alpha}\frac{\partial T}{\partial t} \tag{3}$$

where

$$I_1 = (1 - r_f)I_0$$

and r_f is the reflection coefficient, C_1 is the intensity multiplication factor, and I_0 is the peak power intensity.

The initial and boundary conditions are:

- At time $t = 0$

$$T(x, 0) = T_0$$

- At the surface $x = 0$

$$\left[\frac{\partial T}{\partial x}\right]_{x=0} = 0$$

- At $x = \infty$

$$T(\infty, t) = T_0$$

After introducing the dimensionless parameters as

$$\tau = \alpha\delta^2 t \qquad \eta = \delta x \qquad \theta = T\frac{k\delta}{I_1}$$

Equation 3 becomes

$$\frac{\partial^2\theta}{\partial\eta^2} + [C_1 \times SP(\tau)]e^{-\eta} = \frac{\partial\theta}{\partial\tau} \tag{4}$$

where

$$SP(\tau) = 1[\tau] - 1[\tau - \Delta\tau]$$

and $\Delta\tau = \alpha\delta^2\Delta t$ ($\Delta\tau$ is the dimensionless pulse length).

The dimensionless initial and boundary conditions become:

- At time $\tau = 0$

$$\theta(\eta, 0) = \theta_0$$

- At the surface $\eta = 0$

$$\left[\frac{\partial\theta}{\partial\eta}\right]_{\eta=0} = 0$$

- At $\eta = \infty$

$$\theta(\infty, \tau) = \theta_0$$

The solution of Eq. 4 can be obtained through a Laplace transformation method; that is, with respect to τ, the Laplace transformation of Eq. 4 yields:

$$\frac{\partial^2\bar{\theta}}{\partial\eta^2} - s\bar{\theta} = -[C_1 \times SP(s)]e^{-\eta} - \theta_0 \tag{5}$$

Equation 5 has homogeneous and particular solutions. The homogeneous solution of Eq. 5 can be written as

$$\bar{\theta}_h = K_1 e^{\sqrt{s}\eta} + K_2 e^{-\sqrt{s}\eta} \tag{6}$$

and the particular solution for Eq. 5 is

$$\bar{\theta}_p = \frac{[C_1 \times SP(s)]}{s-1}e^{-\eta} + \frac{\theta_0}{s} \tag{7}$$

Therefore, the solution of dimensionless temperature in the Laplace domain becomes

$$\bar{\theta} = K_1 e^{\sqrt{s}\eta} + K_2 e^{-\sqrt{s}\eta} + \frac{[C_1 \times SP(s)]}{s-1}e^{-\eta} + \frac{\theta_0}{s} \tag{8}$$

The boundary condition $\theta(\infty, \tau) = \theta_0$ results in $K_1 = 0$. The boundary condition at the surface yields

$$\left[\frac{\partial\theta}{\partial\eta}\right]_{\eta=0} = \left[-K_2 e^{-\sqrt{s}\eta}\sqrt{s} - \frac{[C_1 \times SP(s)]}{s-1}e^{-\eta}\right]_{\eta=0} = 0$$

which results in

$$K_2 = -\frac{[C_1 \times SP(s)]}{\sqrt{s}\,(s-1)}$$

Therefore, Eq. 8 becomes

$$\bar{\theta} = -\frac{[C_1 \times SP(s)]}{\sqrt{s}\,(s-1)}e^{-\sqrt{s}\eta} + \frac{[C_1 \times SP(s)]}{(s-1)}e^{-\eta} + \frac{\theta_0}{s} \tag{9}$$

Noting from Eq. 1 that

$$SP(s) = \frac{1}{s} - \frac{e^{-(\Delta\tau)s}}{s}$$

Equation 9 thus becomes

$$\bar{\theta} = -C_1\left\{\frac{e^{-\sqrt{s}\eta}}{s\sqrt{s}\,(s-1)} - \frac{e^{-\sqrt{s}\eta-(\Delta\tau)s}}{s\sqrt{s}\,(s-1)}\right\} + C_1\left\{\frac{e^{-\eta}}{s(s-1)} - \frac{e^{-\eta-(\Delta\tau)s}}{s(s-1)}\right\} + \frac{\theta_0}{s} \tag{10}$$

Noting that

$$\frac{1}{s(s-1)} = \frac{1}{s-1} - \frac{1}{s}$$

The inversion of Laplace transforms can be written as

$$\mathfrak{L}^{-1}\left[\frac{e^{-\sqrt{s}\eta}}{s\sqrt{s}\,(s-1)}\right] = \mathfrak{L}^{-1}\left[\frac{e^{-\sqrt{s}\eta}}{\sqrt{s}\,(s-1)}\right] - \mathfrak{L}^{-1}\left(\frac{e^{-\sqrt{s}\eta}}{s\sqrt{s}}\right)$$

$$\mathfrak{L}^{-1}\left[\frac{e^{-\eta}}{s(s-1)}\right] = \mathfrak{L}^{-1}\left[\frac{e^{-\eta}}{(s-1)}\right] - \mathfrak{L}^{-1}\left(\frac{e^{-\eta}}{s}\right)$$

Consequently, the Laplace transformation of $\mathfrak{L}^{-1}[e^{-\sqrt{s}\eta}/s\sqrt{s}(s-1)]$ yields[21]

$$\mathfrak{L}^{-1}\left[\frac{e^{-\sqrt{s}\eta}}{s\sqrt{s}\,(s-1)}\right] = \frac{e^{\tau}}{2}\left[e^{-\eta}\mathrm{erfc}\left(-\sqrt{\tau}+\frac{\eta}{2\sqrt{\tau}}\right) - e^{\eta}\mathrm{erfc}\left(\sqrt{\tau}+\frac{\eta}{2\sqrt{\tau}}\right)\right] - \left[\frac{2\sqrt{\tau}}{\sqrt{\pi}}e^{-(\eta^2/4\tau)} - \eta\,\mathrm{erfc}\left(\frac{\eta}{2\sqrt{\tau}}\right)\right] \quad (11)$$

Let's denote the righthand side of Eq. 11 $f(\eta, \tau)$. Consider the following Laplace operation:

$$\mathfrak{L}^{-1}e^{-\Delta s}F(s) = f(t-\Delta t)$$

where

$$\mathfrak{L}^{-1}F(s) = f(t)$$

Therefore

$$\mathfrak{L}^{-1}e^{-\Delta s}\left[\frac{e^{-\sqrt{s}\eta}}{s\sqrt{s}\,(s-1)}\right] = f(\eta, \tau-\Delta\tau)$$

Consequently

$$\mathfrak{L}^{-1}\left[e^{-\Delta s}\frac{e^{-\sqrt{s}\eta}}{s\sqrt{s}\,(s-1)}\right] = \frac{e^{\tau-\Delta\tau}}{2}\left[e^{-\eta}\mathrm{erfc}\left(-\sqrt{\tau-\Delta\tau}+\frac{\eta}{2\sqrt{\tau-\Delta\tau}}\right) - e^{\eta}\mathrm{erfc}\left(\sqrt{\tau-\Delta\tau}+\frac{\eta}{2\sqrt{\tau-\Delta\tau}}\right)\right] - \left[\frac{2\sqrt{\tau-\Delta\tau}}{\sqrt{\pi}}e^{-[\eta^2/4(\tau-\Delta\tau)]} - \eta\,\mathrm{erfc}\left(\frac{\eta}{2\sqrt{\tau-\Delta\tau}}\right)\right] \quad (12)$$

Table 1. Pulse Properties Used in the Present Study

$\Delta\tau$	C_1
5, 10	1, 0.5

The Laplace transformation of $\mathfrak{L}^{-1}[e^{-\eta}/s(s-1)]$ yields

$$\mathfrak{L}^{-1}\left[\frac{e^{-\eta}}{s(s-1)}\right] = e^{-\eta}[e^{\tau}-1(\tau)] \quad (13)$$

where $1(\tau)$ is a unit step function.

Similarly,

$$\mathfrak{L}^{-1}\left[e^{-\Delta s}\frac{e^{-\eta}}{s(s-1)}\right] = e^{-\eta}[e^{\tau-\Delta\tau}-1(\tau-\Delta\tau)] \quad (14)$$

Using the terms in Eqs. 11–14, the dimensionless temperature (Laplace inversion of Eq. 10) becomes

$$\theta = \theta_o + C_1\left\{\begin{array}{c} e^{-\eta}[e^{\tau}-1(\tau)] \\ -\frac{e^{\tau}}{2}\left[\begin{array}{c} e^{-\eta}Erfc(-\sqrt{\tau}+\frac{\eta}{2\sqrt{\tau}}) \\ -e^{\eta}Erfc(\sqrt{\tau}+\frac{\eta}{2\sqrt{\tau}}) \end{array}\right] \\ +\left[\frac{2\sqrt{\tau}}{\sqrt{\pi}}e^{-\frac{\eta^2}{4\tau}} - \eta Erfc(\frac{\eta}{2\sqrt{\tau}})\right] \end{array}\right\} - C_1\left\{\begin{array}{c} e^{-\eta}[e^{\tau-\Delta\tau}-1(\tau-\Delta\tau)] \\ -\frac{e^{\tau-\Delta\tau}}{2}\left[\begin{array}{c} e^{-\eta}Erfc(-\sqrt{\tau-\Delta\tau}+\frac{\eta}{2\sqrt{\tau-\Delta\tau}}) \\ -e^{\eta}Erfc(\sqrt{\tau-\Delta\tau}+\frac{\eta}{2\sqrt{\tau-\Delta\tau}}) \end{array}\right] \\ +\left[\frac{2\sqrt{\tau-\Delta\tau}}{\sqrt{\pi}}e^{-\frac{\eta^2}{4(\tau-\Delta\tau)}} - \eta Erfc(\frac{\eta}{2\sqrt{\tau-\Delta\tau}})\right] \end{array}\right\} \quad (15)$$

Equation 15 is developed for a step intensity pulse starting at $\tau = 0$ and ending at $\tau = \Delta\tau$, where $\Delta\tau$ is a pulse length, with amplitude multiplication factor of C_1 as shown in Figure 1.

The pulse properties used in the computation are given in Table 1.

Entropy analysis

Volumetric entropy generation rate in a thermal system can be written as[22]

$$\dot{S}_{gen} = \frac{1}{T}\nabla\cdot q - \frac{1}{T^2}q\nabla T + \rho\frac{DS}{Dt} \quad (16)$$

where

$$\rho \frac{DS}{Dt} = \frac{\rho}{T}\frac{Du}{Dt} - \frac{P}{\rho T}\frac{D\rho}{Dt} \tag{17}$$

Because the density remains constant for solids, the second term in Eq. 17 reduces to zero [that is, $(P/\rho T)(D\rho/Dt)$]. Consequently, Eq. 16 can now be expressed as

$$\dot{S}_{gen} = \frac{1}{T}\nabla \cdot q - \frac{1}{T^2} q\nabla T + \frac{\rho}{T}\frac{Du}{Dt} \tag{18}$$

The term $(\rho/T)(Du/Dt)$ in a one-dimensional (1-D) solid can be written as

$$\frac{\rho}{T}\frac{Du}{Dt} = \frac{1}{T}(-\nabla \cdot q) \tag{19}$$

Combining Eqs. 18 and 19 yields

$$\dot{S}_{gen} = \frac{1}{T}\nabla \cdot q - \frac{1}{T^2} q\nabla T + \frac{1}{T}(-\nabla \cdot q) \tag{20}$$

where $q = -k\nabla T$. Therefore, rearrangement of Eq. 20 yields

$$\dot{S}_{gen} = \frac{k}{T^2}(\nabla T)^2 \tag{21}$$

In terms of the dimensionless quantities, the dimensionless volumetric entropy generation rate is

$$\dot{S}^*_{gen} = \frac{1}{\theta^2}(\nabla \theta)^2 \tag{22}$$

where

$$\dot{S}^*_{gen} = \dot{S}_{gen}\frac{1}{k\delta}$$

Equation 22 can be used to formulate the volumetric entropy generation rate during the heating and cooling cycles of the laser-heating pulse.

Consider the following relations:

$$\frac{d}{d\eta}[\mathrm{erfc}(z)] = -\frac{2}{\sqrt{\pi}} e^{-z^2}\frac{dz}{d\eta}$$

$$\frac{d}{d\eta}[\mathrm{erf}(z)] = \frac{2}{\sqrt{\pi}} e^{-z^2}\frac{dz}{d\eta}$$

$$\frac{d}{d\eta}\left[\mathrm{erf}\left(a + \frac{z}{b}\right)\right] = -\frac{2}{b\sqrt{\pi}} e^{-[a+(x/b)]^2}\frac{dz}{d\eta} \tag{23}$$

$\nabla\theta$ can be obtained from Eq. 15 by introducing the system of expressions in Eq. 23, that is,

$$\begin{aligned}
\nabla\theta \;=\; & C_1 \left\{ \begin{array}{c} -e^{-\eta}[e^{\tau} - 1(\tau)] \\ -\frac{e^{\tau}}{2}\left[\begin{array}{c} -e^{-\eta}Erfc(-\sqrt{\tau} + \frac{\eta}{2\sqrt{\tau}}) - \frac{e^{-\eta}}{\sqrt{\pi}\sqrt{\tau}} e^{-(-\sqrt{\tau}+\frac{\eta}{2\sqrt{\tau}})^2} \\ +e^{-\eta}Erfc(\sqrt{\tau} + \frac{\eta}{2\sqrt{\tau}}) + \frac{e^{-\eta}}{\sqrt{\pi}\sqrt{\tau}} e^{-(\sqrt{\tau}+\frac{\eta}{2\sqrt{\tau}})^2} \end{array} \right] \\ -\frac{\eta}{\sqrt{\tau}\sqrt{\pi}} e^{-\frac{\eta^2}{4\tau}} - \left[Erfc(\frac{\eta}{2\sqrt{\tau}}) - \eta(\frac{1}{\sqrt{\pi}\sqrt{\tau}} e^{-\frac{\eta^2}{4\tau}}) \right] \end{array} \right\} \\
& -C_1 \left\{ \begin{array}{c} -e^{-\eta}[e^{\tau-\Delta\tau} - 1(\tau - \Delta\tau)] \\ -\frac{e^{\tau-\Delta\tau}}{2}\left[\begin{array}{c} -e^{-\eta}Erfc(-\sqrt{\tau - \Delta\tau} + \frac{\eta}{2\sqrt{\tau-\Delta\tau}}) - \frac{e^{-\eta}}{\sqrt{\pi}\sqrt{\tau-\Delta\tau}} e^{-(-\sqrt{\tau-\Delta\tau}+\frac{\eta}{2\sqrt{\tau-\Delta\tau}})^2} \\ +e^{-\eta}Erfc(\sqrt{\tau - \Delta\tau} + \frac{\eta}{2\sqrt{\tau-\Delta\tau}}) + \frac{e^{-\eta}}{\sqrt{\pi}\sqrt{\tau-\Delta\tau}} e^{-(\sqrt{\tau-\Delta\tau}+\frac{\eta}{2\sqrt{\tau-\Delta\tau}})^2} \end{array} \right] \\ -\frac{\eta}{\sqrt{\tau-\Delta\tau}\sqrt{\pi}} e^{-\frac{\eta^2}{4\tau-\Delta\tau}} - \left[Erfc(\frac{\eta}{2\sqrt{\tau-\Delta\tau}}) - \eta(\frac{1}{\sqrt{\pi}\sqrt{\tau-\Delta\tau}} e^{-\frac{\eta^2}{4\tau-\Delta\tau}}) \right] \end{array} \right\}
\end{aligned} \tag{24}$$

Equations 24 and 15 are substituted in Eq. 22 to obtain the volumetric entropy generation rate during the heating and cooling cycles of the laser pulse.

The efficiency of the process may be presented as the ratio of availabilities.[14] In this case, the entropy generation number (*Ns*) can be introduced,[14] that is,

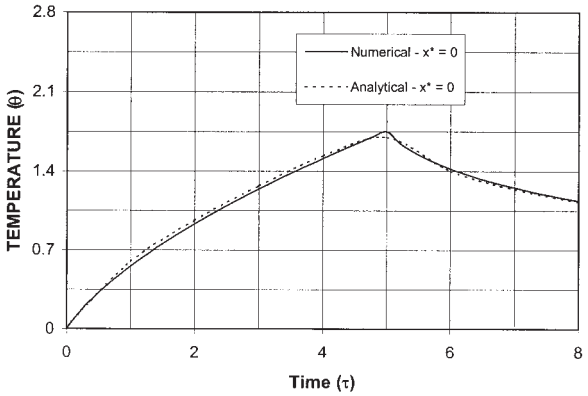

Figure 2. Temporal variation of dimensionless surface temperature obtained from the present study and numerical solutions.

$$Ns = \frac{\text{Total availability destroyed during the process}}{\text{Total availability that enters the system during the process}}$$

Using the Gouy–Stodola theorem,[12] which states that the availability destroyed (A_T) is proportional to the entropy generated, the rate of volumetric availability destroyed in the heating and cooling cycles can be written as

$$\text{In the heating period (for } \tau \le \Delta\tau) \Rightarrow [A_{Tdestroyed}]_{Heating} = \theta_0[\dot{S}^*_{gen}]_{Heating}$$

$$\text{In the cooling period (for } \tau > \Delta\tau) \Rightarrow [A_{Tdestroyed}]_{Cooling} = \theta_0[\dot{S}^*_{gen}]_{Cooling} \quad (25)$$

where $\theta_0 = T_0(k\delta/I_0)$ and T_0 is the reference temperature.

The total availability entering the system (A_{Tin}) during the laser-heating process is the laser energy being absorbed by the substrate material, that is,

$$A_{Tin} = C_1 \int_0^\infty e^{-\eta} d\eta \quad (26)$$

Therefore, the entropy generation number becomes

$$(Ns)_{Heating} = \frac{[A_T]_{Heating}}{A_{Tin}}$$

$$(Ns)_{Cooling} = \frac{[A_T]_{Cooling}}{A_{Tin}} \quad (27)$$

To assess the total availability generated in the heating and cooling cycles, the ratio of entropy generation number (Ns_{ratio}) can be introduced as

$$Ns_{ratio} = \frac{(Ns)_{Heating}}{(Ns)_{Cooling}} \quad (28)$$

Equations 22 and 28 are used to compute the dimensionless volumetric entropy generation rate and the entropy generation number ratio for two pulses with the same energy content, but different pulse lengths.

Results and Discussion

The laser-pulse heating of a solid substrate is modeled and closed-form solutions for temperature rise and entropy generation during the heating and cooling cycles are obtained. The closed-form solutions are presented in nondimensional forms. To investigate the influence of the pulse length on the entropy generation, two pulses with the same energy content, but different pulse lengths, are considered.

Figure 2 shows the temporal variation of dimensionless surface temperature obtained from the present study and nu-

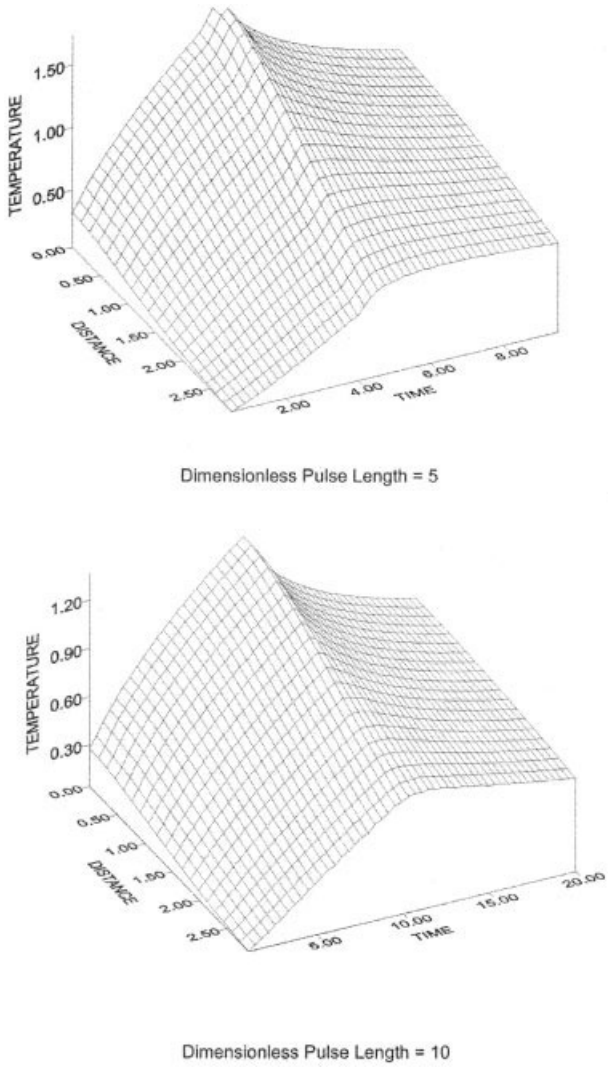

Figure 3. 3-D view of dimensionless temperature for two dimensionless pulse lengths.

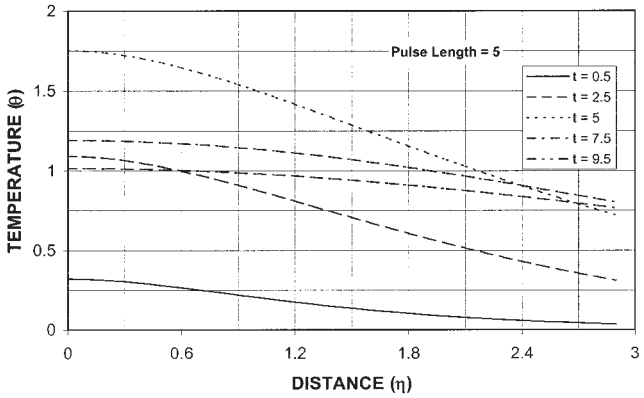

Figure 4. Dimensionless temperature distribution inside the substrate material at different dimensionless times (*t* represents τ) for pulse length = 5.

merical simulations. It can be observed that both profiles are in good agreement.

Figure 3 shows the 3-D plot of dimensionless temperature distribution for two pulse lengths. The magnitude of the maximum temperature for long pulse ($\Delta\tau = 10$) is less than its counterpart corresponding to the short pulse ($\Delta\tau = 5$), that is, the maximum temperature in dimensional form is in the order of 1200°C at the surface. It should be noted that the pulse length of $\Delta\tau = 5$ corresponds to the dimensional pulse length of 10 ns, which is explained by the high power intensity of the short pulse, given that both pulses have the same energy content. Figure 4 shows dimensionless temperature profiles inside the substrate material for the short pulse. The maximum temperature occurs at the pulse end and temperature profiles in the heating cycle ($\tau \leq 5$) decays sharply in the substrate material because of the energy-exchange mechanism. In this case, the internal energy gain increases in the surface region, particularly $\eta \leq 1$ during the heating cycle.

It should be noted that the absorption of the incident laser beam takes place mainly in the region limited to the absorption depth of the substrate material (Lambert's law). Moreover, the insulated boundary condition at the surface ($\partial\theta/\partial\eta = 0$ at $\eta = 0$) eliminates the heat transfer from the free surface. Consequently, the temperature gradient in the surface vicinity decays gradually, but decays sharply in the region next to the surface vicinity. It should be noted that the maximum magnitude of temperature gradient in dimensional form is in the order of 6.5×10^7°C/m. In the cooling cycle, the energy gain from the irradiated field ceases because the cooling cycle starts immediately after the laser pulse ends. Therefore, diffusional energy transport arising from the temperature gradient is the dominating mechanism governing the energy transport process. Consequently, energy transfer from the surface to the solid bulk slows down in the cooling cycle.

In the case of a long pulse scenario, as shown in Figure 5, similar arguments are applicable to those made for Figure 4, provided that the magnitude of maximum temperature is lower in the long pulse case compared to that corresponding in the short pulse case. The depth corresponding to minimum $\partial\theta/\partial\eta$ represents the point where the energy balance attains among the energy absorbed, internal energy gain, and conduction losses such that the rate of internal energy gain becomes gradual.[6] Moreover, the point of minimum $\partial\theta/\partial\eta$ moves away from the surface as the heating period progresses. The diffusional energy transport to the solid bulk resulting from the temperature gradient becomes important beyond the point of minimum $\partial\theta/\partial\eta$. Because the absorption takes place during the long duration for the long pulse, the point of minimum $\partial\theta/\partial\eta$ moves further away from the surface, which can be seen from Figure 5b, in which the temperature gradient is shown. In this case, the temperature gradient changes gradually in the surface region.

Figure 6 shows the temporal variation of dimensionless temperature at different locations inside the substrate material for two pulse lengths. The temperature increases in the early heating period and as the heating period progresses the rate of temperature rise slows, which is more pronounced for the short pulse. This occurs because of the internal energy gain of the substrate material and low diffusional energy transport from the surface vicinity to the solid bulk attributed to the low-temperature gradient in the early heating period. In the cooling cycle, the temperature decays gradually with the progression of

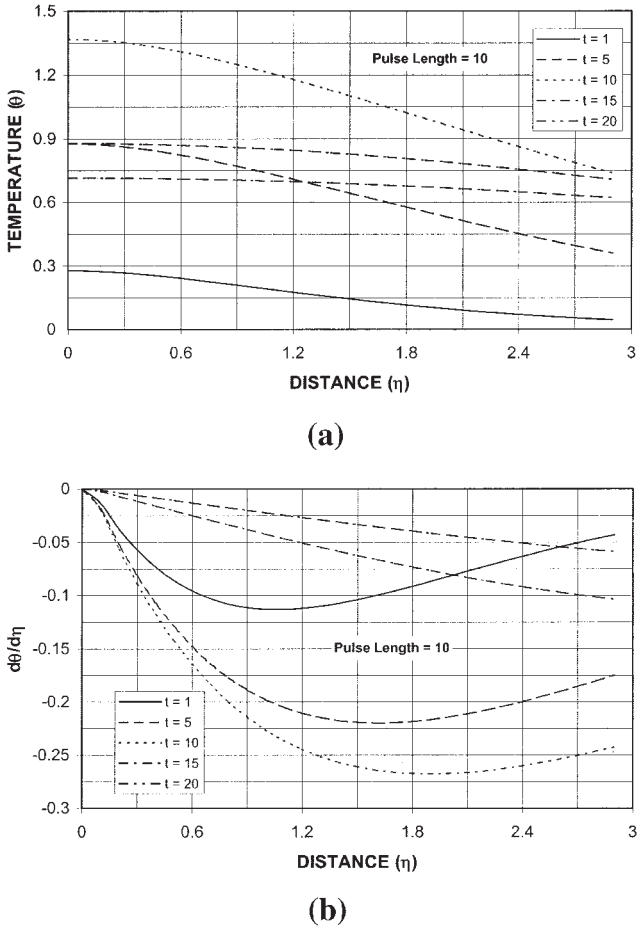

Figure 5. (a) Dimensionless temperature distribution inside the substrate material at different dimensionless times (*t* represents τ) for pulse length = 10; (b) dimensionless temperature gradient inside the substrate material at different dimensionless times (*t* represents τ) for pulse length = 10.

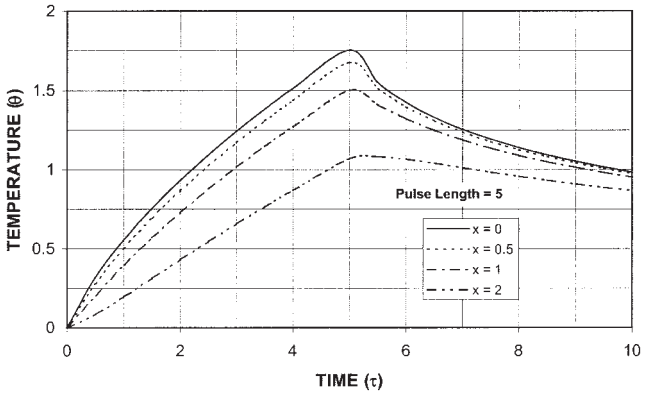

Figure 6. Temporal variation of dimensionless temperature at different dimensionless locations inside the substrate material (*x* represents η) for pulse length = 5.

time because the energy is transported from the surface vicinity to the solid bulk through the diffusional energy transport; that is, absorption is replaced by the diffusional energy transport. The temperature profiles in the region irradiated by a laser beam ($\eta \leq 1$) are closer to each other in the heating cycle; however, it differs at a depth $\eta = 2$. Again, this is attributed to the absorption process, which is negligibly small once the depth increases beyond the absorption depth of the substrate material.

Figure 7 shows a 3-D view of the dimensionless entropy distribution inside the substrate material, whereas Figures 8a and 8b show the dimensionless entropy distributions inside the substrate material at different heating periods and for two pulses. Entropy generation in the surface region is very low, particularly in the surface region, and it is zero at the surface. This is because of the consideration of zero temperature gradient at the surface ($\partial\theta/\partial\eta = 0$ at $\eta = 0$, boundary condition). Moreover, low entropy generation in the surface region arises from the low-temperature gradient in this region. Entropy generation is maximum at the point when the pulse ends. Again this arises from attainment of the high-temperature gradient at the end of the pulse (Figure 3b). Entropy generation is higher in the heating cycle than that in the cooling cycle. Considerable internal energy gain from the irradiated field is responsible for the sharp change of temperature gradient in the region irradiated by a laser beam. In the cooling cycle, entropy generation is less because of the low-temperature gradient. The diffusional energy transport is the sole mechanism governing the energy transport process in this cycle. In a comparison of Figures 8a and 8b, entropy generation is greater for the short pulse than that for the long pulse. In this case, the high intensity of the short pulse results in a sharp change of temperature gradient inside the substrate material, particularly in the region limited to the absorption depth of the substrate material.

Figures 9a and 9b show the entropy number ratio [$(Ns)_{Heating}/(Ns)_{Cooling}$ is the ratio of entropy number in the heating cycle to entropy number in the cooling cycle] inside the substrate material for two pulse lengths. It should be noted that the shift between the time period in the heating and cooling cycles is equal to the pulse length: $(Ns)_{Heating}$ corresponds to a time period of 1 in the heating cycle, whereas $(Ns)_{Cooling}$ corresponds to the time period of 6 in the cooling cycle for the short pulse. $(Ns)_{Heating}/(Ns)_{Cooling}$ attains values > 1 as a result of the high level of entropy generation in the heating cycle. Moreover, $(Ns)_{Heating}/(Ns)_{Cooling}$ attains high values in the surface region despite the fact that entropy generation is low in this region for both cycles, which indicates that the insulated boundary condition at the surface results in relatively higher entropy generation in the heating cycle than that in the cooling cycle in this region. As the depth from the surface increases, $(Ns)_{Heating}/(Ns)_{Cooling}$ decreases, indicating that the entropy generation in both cycles is similar in this region. When comparing Figures 9a and 9b, it can be observed that $(Ns)_{Heating}/(Ns)_{Cooling}$ corresponding to the short pulse is lower than its counterpart corresponding to the long pulse, even though the entropy generation for the short pulse is higher than that for the long pulse, particularly in the heating cycle. The possible explanation for this situation is that the amount of entropy generation in cooling and heating cycles for a long pulse differs substantially, which in turn increases $(Ns)_{Heating}/(Ns)_{Cooling}$.

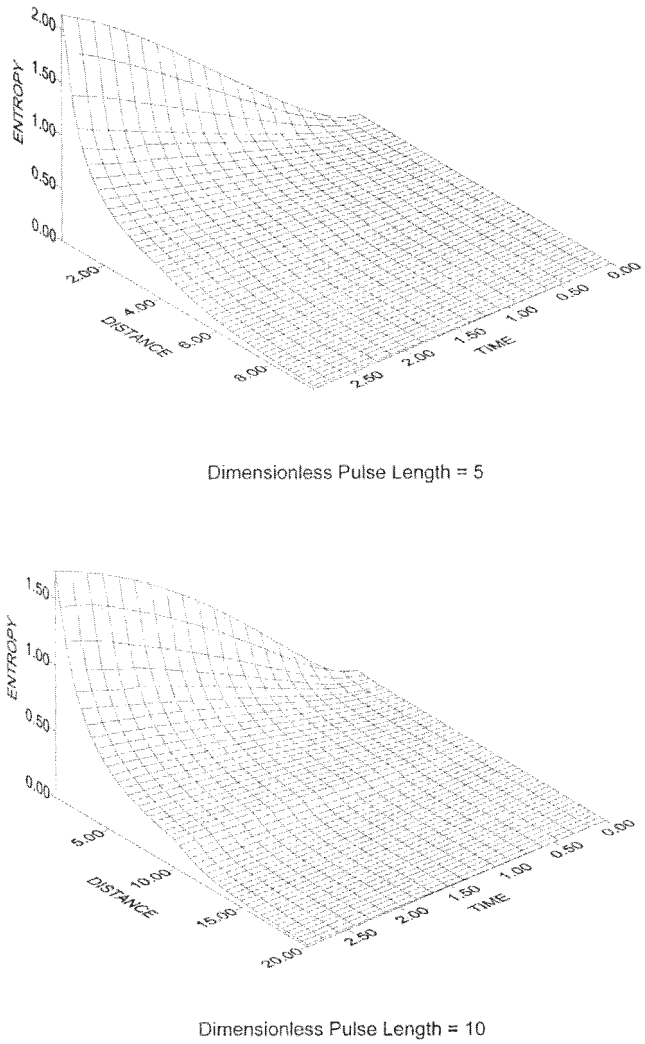

Figure 7. 3-D view of dimensionless entropy generation for two pulse lengths.

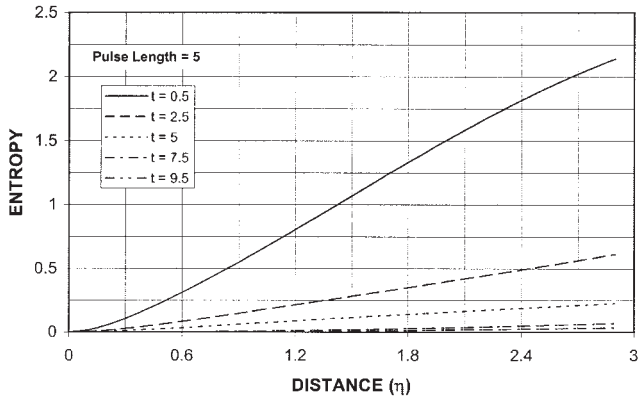

(a)

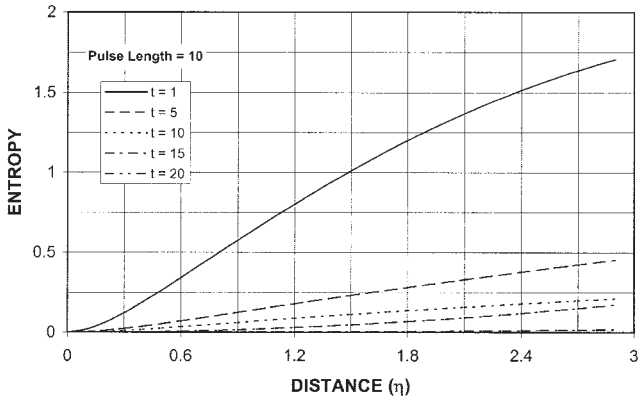

(b)

Figure 8. Dimensionless entropy distribution inside the substrate material at different dimensionless times (*t* represents τ) for (a) pulse length = 5 and (b) pulse length = 10.

Conclusions

Laser-pulse heating of a solid substrate is considered. The nondimensional forms of closed-form solutions for temperature and entropy distributions inside the substrate material are presented. The closed-form solutions are obtained for both heating and cooling cycles of the heating process using a Laplace transformation method. The entropy number ratio $[(Ns)_{Heating}/(Ns)_{Cooling}]$ inside the substrate material is also presented. It is found that the temperature gradient gradually decays in the surface vicinity of the substrate material as a result of not only an insulated boundary condition at the surface but also a substantial increase of the internal energy from the irradiated field in this region. Entropy generation in the region irradiated by a laser beam is higher for a short pulse duration than that corresponding to a large pulse duration, provided that both pulses have the same energy content. This indicates that laser heating with long pulse lengths results in less entropy generation in the surface vicinity. Moreover, energy losses through a diffusional process from the surface region toward the solid bulk, arising from the temperature gradient, become less for long pulses as observed from the entropy generation. Consequently, for the practical application of laser-conduction limited-heating situations, the laser pulse with long pulse lengths should be favorable. The specific conclusions derived from the present study are as follows:

(1) Temperature rises rapidly in the early heating period of the heating cycle as a result of the substantial energy gain from the irradiated field. Once the laser pulse terminates, the temperature gradually decays in the substrate material. In this case, diffusional energy transfer is the sole mechanism governing the energy transport inside the substrate material.

(2) Entropy generation is higher in the heating cycle than that in the cooling cycle, which is explained by attainment of a high-temperature gradient in the heating cycle; that is, considerable internal energy gain is responsible for the sharp change in temperature gradient inside the substrate material. Entropy generation arising from the short pulse is greater than its counterpart corresponding to the long pulse. In this case, the short pulse has a higher pulse intensity than that of the long pulse because both pulses have the same energy content.

(3) Entropy number ratio $[(Ns)_{Heating}/(Ns)_{Cooling}]$ is higher in the surface vicinity of the substrate material despite the low entropy generation in this region. This indicates that the entropy generation in the surface region is considerably low in the cooling cycle because of (i) the insulated boundary condition at

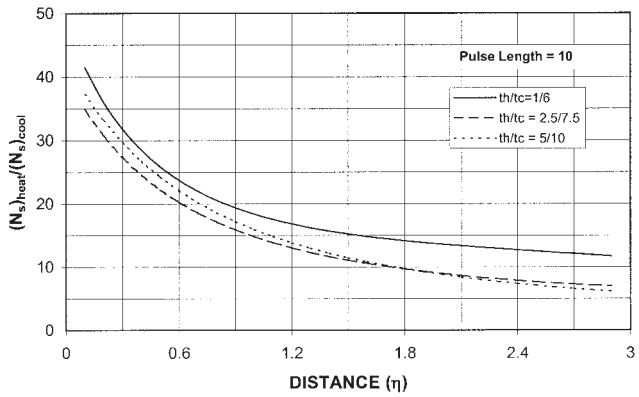

(a)

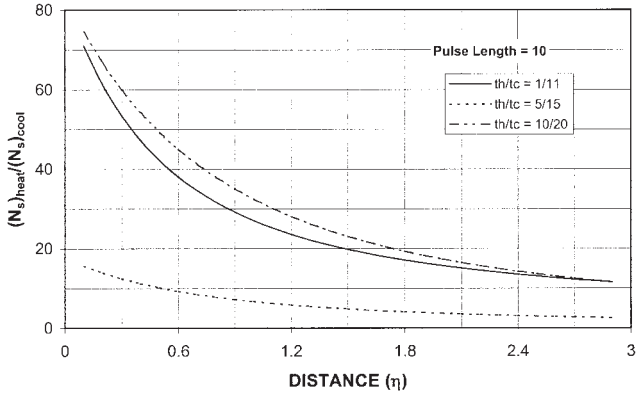

(b)

Figure 9. Entropy number ratio distribution inside the substrate material at different dimensionless time ratios (*th*, heating period; *tc*, cooling period) for (a) pulse length = 10.

the surface and (ii) the energy gain from the irradiated field ceases after the pulse ends and the diffusional energy transfer becomes the sole mechanism governing the energy transport process inside the substrate material. Entropy number ratio is higher for the long pulse than that for the short pulse, which indicates that the entropy generation in the cooling cycle for the long pulse is considerably smaller than its counterpart corresponding to the heating cycle.

Acknowledgments

The authors acknowledge support of this work from King Fahd University of Petroleum and Minerals, Dhahran, Saudi Arabia.

Notation

A_T = dimensionless total availability destroyed
Cp = specific heat, J kg^{-1} K^{-1}
C_1 = intensity multiplication factor
I_1 = power intensity $[I_0(1 - r_f)]$, W/m^2
I_0 = laser peak power intensity, W/m^2
k = thermal conductivity, W m^{-1} K^{-1}
Ns = entropy generation number
P = pressure, Pa
s = Laplace variable
$\dot{S}_{gen}$ = volumetric entropy generation rate, W m^{-3} K^{-1}
$\dot{S}^*_{gen}$ = dimensionless volumetric entropy generation rate
r_f = reflection coefficient
t = time, s
Δt = pulse length of laser pulse, s
T_0 = ambient temperature, K
$T(x, t)$ = temperature, K
u = internal energy, J
x = spatial coordinates corresponding to the x-axis, m

Greek letters

α = thermal diffusivity, m^2/s
δ = absorption coefficient, 1/m
η = dimensionless distance $(=x\delta)$
$\theta(\eta, \tau)$ = dimensionless surface temperature $[=T(x, t)(k\delta/I_1)]$
θ_0 = dimensionless ambient temperature $[=T_0(k\delta/I_1)]$
τ = dimensionless time $(=\alpha\delta^2 t)$
$\Delta\tau$ = dimensionless pulse length of laser pulse
ρ = density, kg/m^3

Literature Cited

1. Ready JF. Effects due to absorption of laser radiation. *J Appl Phys.* 1963;36:462-470.
2. Blackwell FJ. Temperature profile in semi-infinite body with exponential source and convective boundary conditions. *ASME J Heat Transfer.* 1990;112:567-571.
3. Lu Y. Square-shaped temperature distribution induced by a Gaussian-shaped laser beam. *Appl Surf Sci.* 1994;81:357-364.
4. El-Adawi MK, Abel-Naby MA, Shalaby S. Laser heating of a two layer system with constant surface absorption: An exact solution. *Int J Heat Mass Transfer.* 1995;38:947-952.
5. Modest MF, Abaikans H. Evaporative cutting of a semi-infinite body with a moving cw laser. *ASME J Heat Transfer.* 1988;108:602-607.
6. Yilbas BS, Shuja SZ. Heat transfer analysis of laser heated surfaces-conduction limited case. *Appl Surf Sci.* 1997;108:167-175.
7. Yilbas BS, Kalyon M. Laser repetitive pulse heating with convective boundary condition at the surface. *J Phys D Appl Phys.* 2001;34:222-231.
8. Yilbas BS. Analytical solution for time unsteady laser pulse heating of semi-infinite solid. *Int J Mech Sci.* 1997;39:671-682.
9. Demirel Y, Sandler SI. Linear-nonequilibrium thermodynamics theory for coupled heat and mass transport. *Int J Heat Mass Transfer.* 2001; 44:2439-2451.
10. Sieniutycz S. Carnot problem of maximum work from a finite resource interacting with environment in a finite time. *Physica A.* 1999;264: 234-263.
11. Carrington G, Sun ZF. Second law analysis of combined heat and mass transfer in internal and external flows. *Int J Heat Fluid Flow.* 1992; 13:65-70.
12. Krane RJ. A second law analysis of the optimum design and operation of thermal energy storage systems. *Int J Heat Mass Transfer.* 1987; 30:43-57.
13. Bejan A. A study of entropy generation in fundamental convective heat transfer. *ASME J Heat Transfer.* 1979;101:718-725.
14. Yilbas BS. Three-dimensional laser heating model and entropy generation consideration. *ASME J Energy Resour Technol.* 1999;121:217-224.
15. Yilbas BS. The validity of Fourier theory of radiation heating of metals. *Res Mech.* 1988;24:377-382.
16. Qiu TQ, Tien CL. Short-pulse laser heating on metals. *Int J Heat Mass Transfer.* 1992;35:719-726.
17. De Groot SR. *Introduction to Thermodynamics of Irreversible Processes*. New York, NY: Wiley; 1962:94.
18. Fitts DD. *Nonequilibrium Thermodynamics*. New York, NY: McGraw-Hill; 1962:41.
19. Katchalsky A, Curran PF. *Nonequilibrium Thermodynamics*. Cambridge, MA: Harvard Univ. Press; 1975:113.
20. Prigogine I. *Introduction to Thermodynamics of Irreversible Processes*. New York, NY: Wiley; 1967:40.
21. Abramowitz M, Stegun IA. *Handbook of Mathematical Functions*. New York, NY: Dover; 1965:1020.
22. Bejan A. *Entropy Generation Minimization*. New York, NY: CRC Press; 1995:74.

Manuscript received Sept. 30, 2005, and revision received Nov. 16, 2005.